

## Superdeformation in $^{191}\text{Au}$

D. T. Vo, W. H. Kelly, F. K. Wohn, and J. C. Hill  
*Iowa State University, Ames, Iowa 50011*

M. A. Deleplanque, R. M. Diamond, F. S. Stephens, J. R. B. Oliveira,\* J. Burde,<sup>†</sup> A. O. Macchiavelli,<sup>‡</sup>  
 J. deBoer,<sup>§</sup> B. Cederwall, I. Y. Lee, and P. Fallon  
*Nuclear Science Division, Lawrence Berkeley Laboratory, Berkeley, California 94720*

J. A. Becker, E. A. Henry, M. J. Brinkman, A. Kuhnert,<sup>||</sup> M. A. Stoyer, and J. R. Hughes  
*Lawrence Livermore National Laboratory, Livermore, California 94550*

J. E. Draper, C. Duyar, and E. Rubel  
*University of California, Davis, California 95616*

(Received 28 December 1992)

A superdeformed band has been observed for the first time in an Au isotope. The reaction used was  $^{11}\text{B} + ^{186}\text{W}$ , demonstrating that very light ions can be used to populate superdeformed (SD) bands at high angular momentum. The band is assigned to  $^{191}\text{Au}$ . The  $\gamma$ -ray energies are at the quarter-point energies of the  $^{192}\text{Hg}$  SD band, indicating that it is "identical" to that of  $^{192}\text{Hg}$ .

PACS numbers: 23.20.Lv, 21.10.Re, 27.80.+w

The search for new superdeformed (SD) bands is important in many respects. Perhaps most obviously, SD bands are a critical test of our ability to predict nuclear properties. Multiple bands in a given nucleus give us information about the orbitals involved at large deformations, which may be quite different from those in normally deformed nuclei. Superdeformed bands are often identical to others in neighboring nuclei and new examples often provide clues that will help us understand this puzzling phenomenon. "Identical" SD bands, usually in different nuclei, refer to rotational bands that have not only the same moment of inertia, but also identical or "equivalent" transition energies. The "equivalent" transition energies correspond to half-points or quarter-points between two consecutive transition energies in the identical band. Since each transition carries two units of angular momentum, this means that any additional single particle contribution to the angular momentum must be half-integer or integer. This is not expected in the "traditional" models and may lead to the development of new concepts and reveal new symmetries.

In the mass 190 region, superdeformed nuclei are known only for the Hg, Tl, and Pb isotopes [1], although they are predicted [2,3] for both higher and lower atomic numbers. In the SD candidate nuclei with  $Z > 82$ , it is very difficult to find new superdeformed bands because of higher fission competition. Prior to this work, no SD bands had been found in this region for  $Z < 80$ . These relatively neutron-rich nuclei can only be populated at high angular momentum with very light neutron-rich projectiles. We report here the first superdeformed band found in a gold ( $Z = 79$ ) nucleus,  $^{191}\text{Au}$ . This SD band is the first experimental evidence that this region of superdeformation extends below  $Z = 80$ . In this odd- $Z$

nucleus, we find that the superdeformed band is "identical" to quarter-point energies of the SD band in the "doubly magic"  $^{192}\text{Hg}$  and to an excited band in  $^{191}\text{Hg}$ , an odd-neutron nucleus. This is different from the behavior of the Tl nuclei, the other odd- $Z$  SD nuclei in this region, where the extra odd proton does not produce a SD band identical to that in  $^{192}\text{Hg}$ .

The experiments were carried out at the Lawrence Berkeley Laboratory 88-Inch Cyclotron using the High Energy-Resolution Array (HERA) facility. HERA consisted of twenty Compton-suppressed Ge detectors and a central 40-element bismuth germanate (BGO) ball. States in  $^{190,191,192}\text{Au}$  were populated in the reaction  $^{186}\text{W}(^{11}\text{B}, xn)$  at three different beam energies: 78, 84, and 86 MeV. The targets consisted of one to three stacked self-supporting 0.5 mg/cm<sup>2</sup>  $^{186}\text{W}$ . All threefold and higher  $\gamma$ -ray coincidences were recorded. The twofold coincidence events were recorded only if they were in coincidence with at least six inner ball detectors. All events were recorded together with the  $\gamma$ -ray sum energy and the multiplicity of the inner ball. Also, in the 86-MeV reaction, the time differences between the  $\gamma$  rays detected in the BGO ball and the first-coincident Ge detector were recorded to enable the rejection of delayed  $\gamma$  rays and neutron-induced events. A total of  $2.0 \times 10^8$ ,  $1.9 \times 10^8$ , and  $3.7 \times 10^8$  double events and  $3.5 \times 10^7$ ,  $4.3 \times 10^7$ , and  $5.0 \times 10^7$  triple and higher coincidence events were recorded for the three runs at 78, 84, and 86 MeV, respectively. In each case Doppler-shift corrections were made on the energies of the  $\gamma$  rays emitted from the recoiling nuclei. In a separate set of experiments, the  $^{176}\text{Yb}(^{19}\text{F}, xn)$  reaction was used at 100- and 105-MeV bombarding energies with a target consisting of three stacked  $^{176}\text{Yb}$  metallic foils of 0.5 mg/cm<sup>2</sup> thick-

ness. Summed over both energies, a total of  $3.4 \times 10^8$  double and  $1.2 \times 10^8$  triple and higher coincidence events were recorded.

Correlation matrices of  $E_\gamma$ - $E_\gamma$  coincidences were constructed with various  $\gamma$ -ray sum-energy ( $H$ ) and multiplicity ( $k$ ) requirements. A channel-by-channel search of the matrices revealed a band of at least 13 transitions from  $E_\gamma = 229$  to 678 keV in the 86-MeV and 84-MeV data sets for the  $^{186}\text{W}(^{11}\text{B},xn)$  reaction (Fig. 1). There is also some weak indication of this band in the 78-MeV data set. The transition indicated by \* in Fig. 1 is found in coincidence with SD band members. It has the same energy (371 keV) as the known low-spin  $13/2^- - 9/2^-$  transition in  $^{191}\text{Au}$  [4]. However, this transition feeds the 10-ns isomer in  $^{191}\text{Au}$ . Because the recoiling nuclei move out of view of the Ge detectors, the 274-keV ( $9/2^- - 11/2^-$ ) and subsequent transitions in the decay of the isomer are not seen. The relative intensity pattern of the band is shown in the inset. The uncertainties are relatively large due to the very weak intensities. The transition intensities, internal conversion included, increase as the transition energies decrease, become relatively constant for energies from 500 keV down to 300 keV, and decrease after that. This intensity pattern is similar to those of the bands in  $^{191}\text{Hg}$  [5]. The energy spacings of the transitions in this band are similar to others in this region, with the differences between adjacent transitions being  $\approx 41$  keV for the lowest energy transitions and  $\approx 34$  keV for the highest energy transitions.

The assignment of the new band to  $^{191}\text{Au}$  is supported

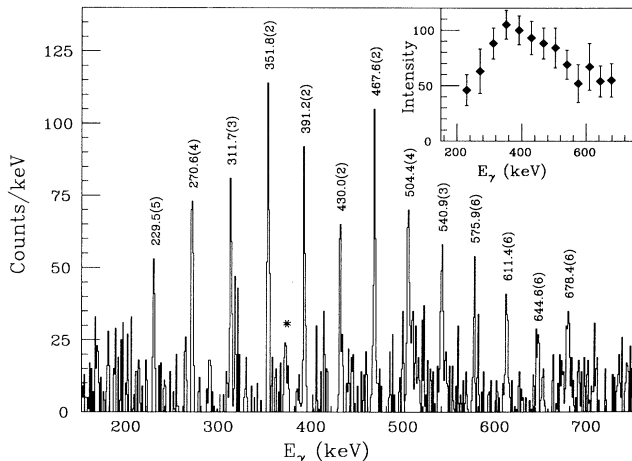


FIG. 1. The  $\gamma$ -ray spectrum of the SD band produced in the  $^{186}\text{W}(^{11}\text{B},6n)^{191}\text{Au}$  reaction. The data represent the sum of the 84-MeV and 86-MeV data sets. This spectrum is obtained by double gating threefold and higher events. For the 84-MeV data set, the gates are nine transitions from 228 keV to 540 keV. The gates for the 86-MeV data set are all 13 band members. The transition indicated by \* is 371 keV (see text). The inset shows the transition intensities, deduced from the double-gated spectrum.

by the excitation function and cross bombardment results. The SD band is much weaker in the 78-MeV reaction data where  $^{192}\text{Au}$  is much more intense (compared with either the 84- or 86-MeV reaction) so that one may rule out the possibility of the SD band belonging to  $^{192}\text{Au}$ . Known states with similar spins were populated in the other experiment,  $^{176}\text{Yb}(^{19}\text{F},xn)$ . The residual nucleus has about the same energy of excitation and maximum angular momentum as those in the  $^{186}\text{W}(^{11}\text{B},6n)$  reaction. The statistics of  $^{190}\text{Au}$  in this reaction are much better while the  $^{191}\text{Au}$  populations are much smaller than those in the  $^{186}\text{W}(^{11}\text{B},xn)$  reaction at 84 and 86 MeV. Careful searches for this SD band were performed in these data and it was not found. This suggests that this SD band most likely belongs to  $^{191}\text{Au}$  and not to  $^{190,192}\text{Au}$ . With a multiplicity  $k \geq 18$  and sum energy  $H \geq 14$  MeV, the band intensity is only 0.15% of the total  $^{191}\text{Au}$  intensity. It is one of the most weakly populated SD bands found to date. There are not sufficient statistics for making a directional correlation analysis to establish multiplicities, and it may be possible that this is a dipole band. However, a plot of the dynamic moments of inertia against frequency ( $\hbar\omega$ ) for this new band compared with similar plots of dipole bands (e.g., in  $^{197}\text{Pb}$  and in  $^{199}\text{Pb}$ ) [6,7] and other SD bands in this region shows a behavior of the dynamic moments of inertia more regular than those of dipole bands and more similar to that of the SD bands. In fact, the band is identical to some other SD bands. Therefore, we made a reasonable assumption that these cascade  $\gamma$  rays of the SD band have multipolarity  $L = 2$ . Because of the weakness of this SD band one might be tempted to assign it to a Pt nucleus produced by a competing ( $^{11}\text{B},pxn$ ) reaction. However, our data show that the amount of the Pt produced by the competing  $pxn$  channel is a factor of about 30 less than the Au. Typically SD bands in this region are populated at  $\approx 1\%$  or less. For the observed SD band to be in Pt, therefore, it would have to be populated at the unusually high 5% level to give the intensity observed. We regard this alternative as unlikely.

In order to compare this SD band to other bands in this mass region, its dynamic moment of inertia is displayed in Fig. 2 together with those of  $^{192}\text{Hg}$  [8,9] and  $^{191}\text{Hg}^*$  (band 3 in Ref. [5]). It is seen that the moment of inertia for  $^{191}\text{Au}$  is very similar to those of the SD bands of  $^{192}\text{Hg}$  and  $^{191}\text{Hg}^*$ . The energy differences between the transitions of  $^{191}\text{Au}$ ,  $^{192}\text{Hg}$ , and  $^{191}\text{Hg}^*$  SD bands are also shown. Except for the lowest and highest energy transitions, all the comparable transitions in the band are within 2 keV of quarter-point energies of the  $^{192}\text{Hg}$  band and those of the  $^{191}\text{Hg}^*$  SD band.

The fact that the transition energies of the SD band are identical to the quarter-point energies of the  $^{192}\text{Hg}$  band implies that the odd proton hole (relative to the  $^{192}\text{Hg}$  core) occurs in an orbital which has a zero or an integer alignment. In addition, the absence of a signature partner band to the  $^{191}\text{Au}$  SD band suggests some

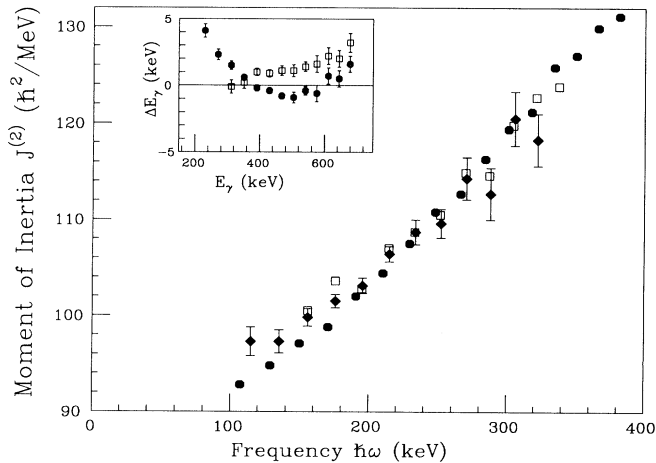


FIG. 2. The dynamic moment of inertia of the  $^{191}\text{Au}$  SD band (diamonds) compared to those in  $^{192}\text{Hg}$  (circles) and  $^{191}\text{Hg}^*$  (squares). The inset shows the energy differences between the bands (circles,  $^{191}\text{Au} - ^{192}\text{Hg}$  quarter-point energies; squares,  $^{191}\text{Au} - ^{191}\text{Hg}^*$ ).

signature splitting. It therefore appears that this band is not based on a strongly coupled orbital.

In order to help assign this odd- $Z$  band to a specific orbital we refer to the single-particle Routhians (Fig. 3). The deformation parameters used to produce this plot were obtained from total Routhian surface (TRS) calculations, based on a deformed Woods-Saxon potential and the Strutinsky shell correction formalism with a monopole pairing interaction [10,11]. Figure 3 shows that at these deformations there are several orbitals near the Fermi surface, including the  $[411]1/2$  and  $[530]1/2$ . Other possibilities are the  $6_2$  and the  $[532]3/2$  orbitals. However, these seem less likely because the  $6_2$  orbital has a changing alignment and the  $[532]3/2$  appears farther away from the Fermi level in these calculations. Both the  $[411]1/2$  and the  $[530]1/2$  orbitals are fairly flat in the observed frequency range. Since a proton hole in a flat orbital will produce no alignment relative to  $^{192}\text{Hg}$ , these assignments are not inconsistent with the observed  $\gamma$  energies. This requires that the decoupling parameter for this orbit be different at these deformations. Indeed particle-rotor model calculations suggest that this may be the case.

The spins of the states are suggested using the methods of Draper *et al.* [12] and Becker *et al.* [13]. Using the two methods to fit the energies of the transitions gives an average of 11.2(1) for the spin parameter of the upper level of the 229-keV transition. Since the nucleus is odd- $A$ , the most likely spin consistent with the above least-squares analysis for the upper level is  $23/2$ .

The alignment plots [14] for  $^{191}\text{Au}$  and  $^{191}\text{Hg}^*$  relative to  $^{192}\text{Hg}$  are displayed in Fig. 4. As with many other examples of superdeformed bands in this region,  $^{191}\text{Au}$  shows an alignment of  $i = 1$  relative to  $^{192}\text{Hg}$ . This gen-

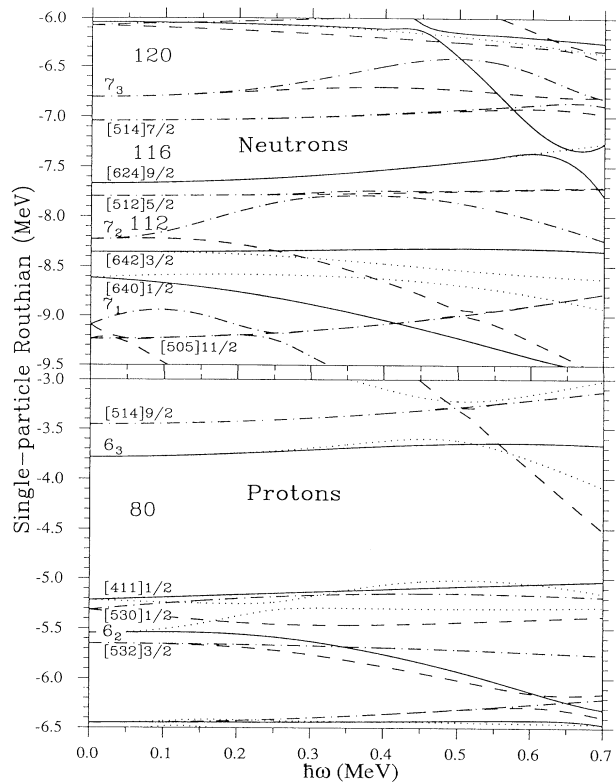


FIG. 3. Single-particle Routhians for  $^{191}\text{Au}$  with deformation parameters  $\beta_2 = 0.457$ ,  $\beta_4 = 0.048$ , and  $\gamma = 0.0$ . The parameters are taken from the lowest SD minimum in the TRS calculations.  $(\pi, \alpha)$ : solid =  $(+, +1/2)$ , dotted =  $(+, -1/2)$ , dash-dotted =  $(-, +1/2)$ , and dashed =  $(-, -1/2)$ .

eral phenomenon is not well understood. However, it has been discussed [14] in terms of the aligned intrinsic pseudospins of a pair of valence nucleons. The weak coupling of the pseudo-orbital to the pseudointrinsic spin is a property of the observed approximate pseudospin symmetry

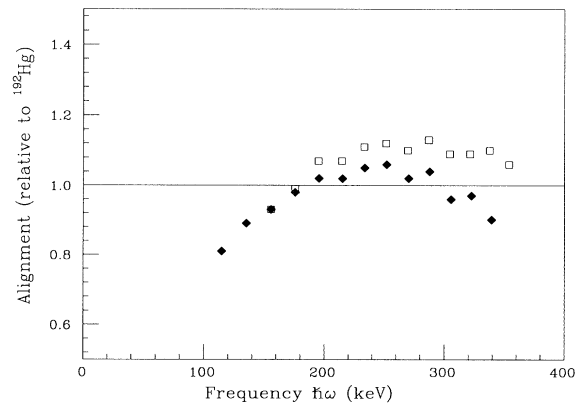


FIG. 4. Alignment of the  $^{191}\text{Au}$  SD band (diamonds) and the  $^{191}\text{Hg}^*$  SD band (squares) relative to the  $^{192}\text{Hg}$  SD band.

in nuclear systems [15].

In addition to the SD band in  $^{191}\text{Au}$  described above, we have observed another somewhat weaker band with energies nearly identical to the yrast SD band in  $^{191}\text{Hg}$  [16]. The transition energies are nearly the same as those in the newly found SD band for low  $E_\gamma$  and they diverge at high  $E_\gamma$ . The energies of the higher energy transitions in this band are 506, 543, 580, 616, 651, and 686 keV. Weak evidence for several of these peaks can be seen in Fig. 1. The peaks are more prominent under different gating conditions. This second band was seen only in the 86-MeV data set and the data are insufficient to allow us to assign it to a nucleus. Because of its apparent relationships to the SD bands of  $^{191}\text{Hg}$  and  $^{191}\text{Au}$ , it would be very interesting to characterize this band further.

In conclusion, we note that the SD band in  $^{191}\text{Au}$  represents the first experimental evidence concerning the nature of the proton orbitals below  $Z = 80$  in superdeformed nuclei. The band may be characterized by either the  $[411]1/2$  or the  $[530]1/2$  proton orbital. This is the first observation of an SD band in this region based on these orbitals. This band has an unexpected and interesting property: it shows an identical band relationship to the yrast (quarter-point energies) band in  $^{192}\text{Hg}$ . However, there is no evidence as yet of a signature partner band. This band is very weak and it represents a limit of what can be done with the current generation of Compton-suppressed Ge arrays. A great deal remains to be learned concerning the properties of this SD region and the relationships between the SD bands. It is important that we continue extending this region of superdeformation with the next generation of detector arrays.

This work is supported in part by the Research Corporation Grant No. R-152 and an IPA Independent Re-

search Agreement with the Division of Undergraduate Education of the National Science Foundation (Kelly), the U.S. Department of Energy under Special Research Grant No. DE-FG02-92ER40692 (ISU), under Contracts No. DE-AC03-76SF00098 (LBL) and No. W-7405-ENG-48 (LLNL), and Grant No. DFG Bo1109 (deBoer).

\* Permanent address: Universidade de São Paulo, São Paulo, SP, Brazil.

† Permanent address: The Racah Institute for Physics, The Hebrew University, Jerusalem, Israel.

‡ Permanent address: Comisión Nacional de Energía Atómica 1429 - Buenos Aires, Argentina.

§ Permanent address: Universität München, Am Coulombwall 1, D - 8046 Garching, Germany.

|| Permanent address: California Institute of Technology, Pasadena, CA 91125.

- [1] R.V.F. Janssens and T.L. Khoo, *Annu. Rev. Nucl. Part. Sci.* **41**, 321 (1991), and references therein.
- [2] R.R. Chasman, *Phys. Lett. B* **219**, 227 (1989).
- [3] S. J. Krieger *et al.*, *Nucl. Phys.* **A542**, 43 (1992).
- [4] Y. Gono *et al.*, *Nucl. Phys.* **A327**, 269 (1979).
- [5] M.P. Carpenter *et al.*, *Phys. Lett. B* **240**, 44 (1990).
- [6] A. Kuhnert *et al.*, *Phys. Rev. C* **46**, 133 (1992).
- [7] G. Baldsiefen *et al.* (to be published).
- [8] J.A. Becker *et al.*, *Phys. Rev. C* **41**, R9 (1990).
- [9] D. Ye *et al.*, *Phys. Rev. C* **41**, 13 (1990).
- [10] R. Wyss *et al.*, *Phys. Lett. B* **215**, 255 (1988).
- [11] W. Nazarewicz *et al.*, *Nucl. Phys.* **A435**, 397 (1985).
- [12] J.E. Draper *et al.*, *Phys. Rev. C* **42**, R1791 (1990).
- [13] J.A. Becker *et al.*, *Phys. Rev. C* **46**, 889 (1992).
- [14] F. Stephens *et al.*, *Phys. Rev. Lett.* **65**, 301 (1990).
- [15] A. Bohr, I. Hamamoto, and Ben R. Mottelson, *Phys. Scr.* **26**, 267 (1982).
- [16] E.F. Moore *et al.*, *Phys. Rev. Lett.* **63**, 360 (1989).